A Stochastic Technique for Multidimensional Granulation Modeling

Justin A. Gantt and Edward P. Gatzke
Dept. of Chemical Engineering, University of South Carolina, Columbia, SC 29208

DOI 10.1002/aic.10911
Published online June 26, 2006 in Wiley InterScience (www.interscience.wiley.com).

Recent granulation modeling research has produced compelling evidence that simple one-dimensional (1-D) models will not suffice when describing the dynamics of particle growth. During the mixing process particles gradually become more saturated due to the loss of air in particles resulting from collisions with the surroundings. This process, called consolidation, influences not only granule pore saturation and binder layer thickness, but also particle coalescence properties. Due to the consolidation behavior observed, a simple size dependent model is typically not adequate. The solution of a multidimensional population balance equation (PBE) is performed using a multiscale solution technique. A microscale model which utilizes a discrete element method (DEM) simulation is used to determine granular flow characteristics and coalescence efficiency. Statistical analysis of data from interactions at the microscale is then used to produce a multidimensional coalescence kernel. Since analytical solutions to PBEs with more than one internal dimension typically do not exist, a constant number kinetic Monte-Carlo (MC) method is used to solve the PBE. This solution technique is used in a test case to model growth of a lactose/starch/HPC and water mixture. The simulated results corresponded well with experimental data. This technique, while in its infancy, proves to be a unique and effective method of bridging multiple scales of the granulation process. © 2006 American Institute of Chemical Engineers *AIChE J,* 52: 3067–3077, 2006

Keywords: population balance, kinetic Monte-Carlo, discrete element method, coalescence kernel

Introduction

Granulation is a particle size enlargement technique where a binder is sprayed onto a powder bed in the presence of some means of bed agitation. Granulation is used in a variety of industries including minerals, pharmaceuticals, food production, detergents and fertilizers. Many particulate process applications demand tight control of particle-size distributions (PSDs) due to requirements on various end-use properties, such as flowability, packing density, drug dissolution rates, and aesthetics. Despite these tight demands, many plants still operate well below capacity and have large recycle ratios due to lack of fundamental knowledge of the process.[1] Models are required for control and optimization of these plants.

Population balance equation models are typically used to model the dynamic progression of PSDs. While aggregation is the primary mechanism present in granulation, it is still poorly understood. It is typically assumed that aggregation occurs following the collision of two particles and is typically described using a rate constant, or kernel. The kernel is often split into two parts, a size independent rate constant β_0, and a size dependent kernel $\beta(u, v)$

$$\beta^*(u, v) = \beta_0\beta(u, v) \tag{1}$$

where u and v are the volumes of the colliding granules.

The size dependent portion of the kernel is represented in

Correspondence concerning this article should be addressed to E. P. Gatzke at gatzke@sc.edu.

© 2006 American Institute of Chemical Engineers

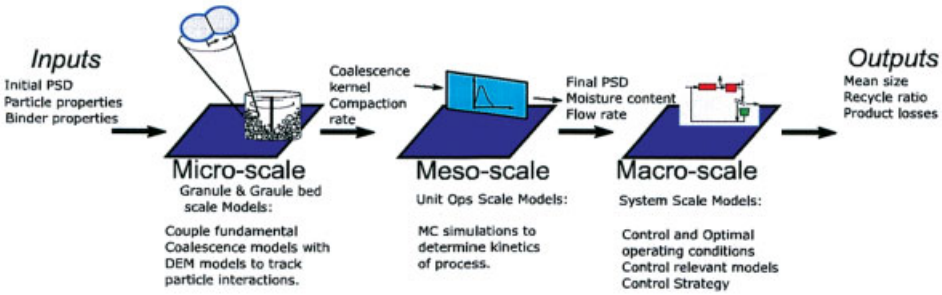

Figure 1. Solution of the multidimensional PBE using a multiscale solution technique.

[Color figure can be viewed in the online issue, which is available at www.interscience.wiley.com.]

many fashions.[1] For instance, Kapur[2] and Sastry[3] used empirical kernels derived from experimental data, and Adetayo and Ennis[4] derived a kernel using Stokes regime analysis to determine a granule size where coalescence was not feasible.

Despite the fact that these kernels are progressing towards more theoretically based models, they still have one glaring limitation: many kernels are only size dependent. Iveson[1] presents a survey of granulation literature which shows that granule porosity, pore saturation, and composition all independently influence granule growth behavior and final product properties. Furthermore, Iveson[5] concludes that 1-D models are unable to account for all of these effects, requiring the development of a multidimensional model.

This article presents an appropriate multidimensional population balance equation model for high-shear granulation. The method of deriving the solution techniques is a multiscale procedure. The process will be analyzed at the granule scale, or microscale, as well as the process scale, or mesoscale. Figure 1 illustrates the multiscale nature of this process. Microscale analysis of the particle-flow behavior and coalescence probability is performed using a discrete element method (DEM) model used in parallel with a coalescence model for deformable, wet granules.[6] A multidimensional coalescence kernel can be derived from statistical analysis of data gathered from the DEM simulation of the process. Mesoscale analysis of the granular rate processes is performed through the use of a multidimensional population balance equation (PBE) which utilizes the derived multidimensional kernel. The PBE is then solved using a kinetic Monte-Carlo (MC) solution technique to determine the dynamic evolution of each multidimensional state (solid, liquid, and air volume). Using this method, the simulation is compared to experimental high-shear granulation data and conclusions are drawn.

Microscale Modeling

Development of a multiscale model for high-shear granulation is presented in this section, where a DEM model is used in parallel with a coalescence model to model particle interactions at the microscale.

Discrete element method (DEM)

Microscale modeling involves the interaction of particles in an agglomerated form. The DEM method is derived from the principles of molecular dynamics (MD). In these simulations, Newton's law of motion is simultaneously solved for a large number discrete particles in a domain used to represent either a control volume with periodic boundaries or an entire vessel. The equations of translational and rotational particle motion are given by

$$m_i \frac{dv_i}{dt} = m_i g + \sum (\mathbf{F}_{Ci} + \mathbf{F}_{wi}) \tag{2}$$

$$I_i \frac{d\omega_i}{dt} = \sum (\mathbf{M}_{Ci} + \mathbf{M}_{wi}) \tag{3}$$

where m_i is the mass of particle i, v_i is the particle velocity vector, g is the gravitational acceleration vector, $\mathbf{F}_{Ci}$ is the sum of the forces on particle i caused by other particles, $\mathbf{F}_{wi}$ is the sum of the forces on particle i caused by the walls of the equipment, I_i is the moment of inertia for particle i, ω_i is the angular velocity of particle i, $\mathbf{M}_{Ci}$ is the sum of the moments on particle i caused by other particles, and $\mathbf{M}_{wi}$ is the sum of the moments on the particle i caused by the walls of the equipment.

The DEM model is used to calculate the collision forces of particles in motion. Note that the DEM does not model agglomeration, it only predicts collision velocities. A model for coalescence of deformable, surface wet granules[7,8] takes into account collision forces, as well as granule and binder properties to determine the likelihood of a successful collision. A soft-sphere DEM model using periodic boundary conditions, and a unique boxing scheme is utilized to simulate velocity-flow fields inside a high-shear mixer.[9,10] These models are in a family of numerical techniques designed for simulating processes which deal with sequential discrete interactions, such as a granulation. They are unique in their ability to replicate the motion of free-flowing granular media. More information regarding DEM modeling techniques is available in 9–14.

Coalescence model

The coalescence model used accounts for the mechanical properties of the particles in motion, as well as the viscous effects of a liquid layer at the surface. Liu et al.[7] define two modes of coalescence based on the collision kinetic energy. *Type I coalescence* results from collisions where the kinetic energy is completely dissipated by the viscous forces of the binder layer. This results in coalescence before the surface collision through the liquid bridge. *Type II coalescence* occurs

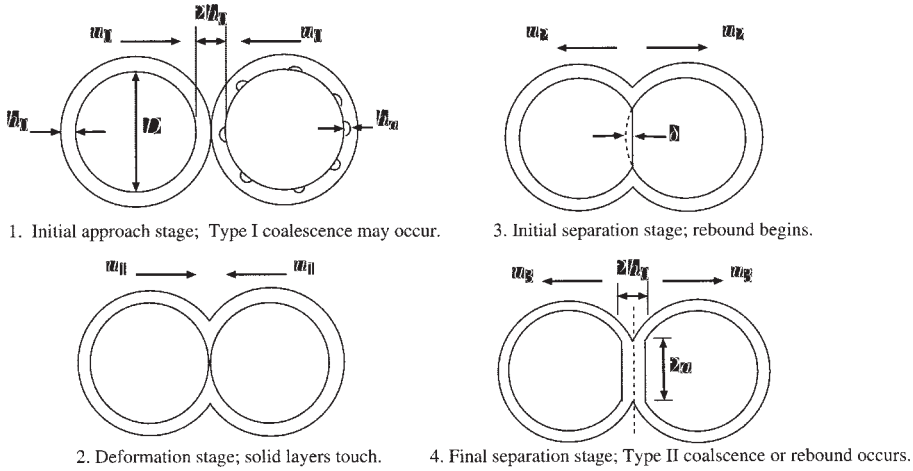

Figure 2. Hertzian based fundamental model for coalescence of deformable, surface wet granules, from Liu et al.[7]

when particles collide and deform, resulting in elastic energy, which cause a retraction of the particles. If the released elastic energy is dissipated by the binder layer, then Type II coalescence occurs, if not, rebound occurs. See Figure 2 for a diagram of this phenomena.

Mesoscale Modeling

The necessity of the incorporation of factors, such as pore saturation, porosity, and moisture content into a population balance requires that other internal parameters in addition to particle size must be considered. A multidimensional population balance which uses solid volume of particles, liquid volume of particles, and air volume of particles as internal coordinates has been proposed by Verkoeijen et al.[15] and Wauters.[16] The benefit of using particle volumes rather than sizes as internal parameters is that volume is conserved, unlike size. In addition, by accounting for solid s, liquid l, and air volume a, one can easily calculate particle diameter $D = 2(3(s + l + a)/(4\pi))^{1/3}$, pore saturation $S = l/(s + l)$, moisture content $w = l/s$, and porosity $\varepsilon = (l + a)/(s + l + a)$. This work utilizes a similar method of deriving the multidimensional particle-density function, and multidimensional birth and death terms as described by Wauters.[16]

Particle density function

This section derives a multidimensional population balance equation which uses solid volume s, liquid volume l, and air volume a, as the internal coordinates. The first step in the derivation of the multidimensional population balance is to define the particle density function n, as a function of solid, liquid, and air volumes. The particle density function is defined as the number of particles N, with an internal solid volume in the interval s to $s + \Delta s$, liquid volume in the interval l to $l + \Delta l$, and air volume in the interval a to $a + \Delta a$. This leads to the following multidimensional integral equation

$$N = \int_{s}^{s+\Delta s} \int_{l}^{l+\Delta l} \int_{a}^{a+\Delta a} n(s, l, a)dsdlda \qquad (4)$$

This number density function is used to track the dynamic transfer of particles from one class to another resulting from coalescence or consolidation. The units for the multidimensional particle density function are $(\#/m^9)$.

Coalescence

Modeling coalescence in multiple dimensions demands additional derivations. Both the birth and death rates must be converted to a multidimensional form. Rather than particles size v and $u - v$ forming a particle of size u, Wauters[16] expanded this relationship as shown in Figure 3. This relationship shows volume is conserved in all dimensions. A particle with a solid volume x coalesces with a particle with a solid volume $p - x$ to form a particle with a solid volume p, as shown in Figure 3. This produces the following birth rate

$$B_{coal} = \frac{1}{2} \int_0^x \int_0^y \int_0^z \Omega(x, y, z, p - x, q - y, r - z) \, n(x, y, z)n(p - x, q - y, r - z)dxdydz \qquad (5)$$

where Ω is the 6-D analog to the 1-D coalescence kernel β. The death rate is defined as

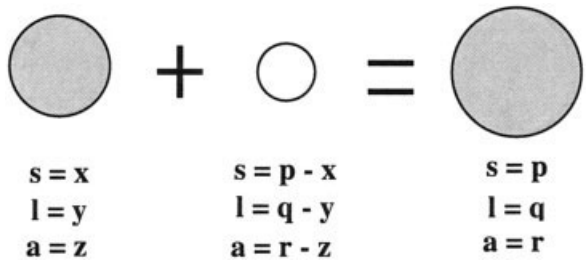

Figure 3. Definition of internal coordinates of birth and death rate following coalescence.

$$D_{coal} = n(p, q, r) \int_0^\infty \int_0^\infty \int_0^\infty \Omega(x, y, z, p, q, r) n(x, y, z) dx dy dz \quad (6)$$

These birth and death rates are then dependent on a multidimensional kernel Ω, which determines how each internal dimension affects the probability of coalescence.

Multiscale Integration

The key to the development of a multiscale model lies within the coalescence kernel. While the coalescence kernel is typically written as the product of a size independent rate constant, and a size dependent term, many of these kernels still require fitting which does not lend itself to a multiscale model. Tan et al.[14] proposed that the kernel should actually be written as the product of a *collision rate* $C_{i,j}$ and the *coalescence efficiency* $\Psi_{i,j}$

$$\beta_{i,j} = C_{i,j} \Psi_{i,j} \quad (7)$$

Ingram[17] points out that this is "the key equation for developing a multiscale model." This equation states that there must be some functional form to describe the particle flow and another form to describe coalescence. While both models are required to provide an estimate at a kernel, these models do not necessarily need to be solved simultaneously. Two models are used at the microscale: a DEM model and the coalescence model.

The key to creating a coalescence kernel which is efficient enough to use at the unit operation scale, yet still incorporate the mechanistic data from the granule and granule bed scale is serial integration of data provided by the DEM/coalescence models to produce a kernel. The data gathered by the DEM/coalescence model will be regressed to form a simple kernel to used at the unit operation scale.

Multiscale analysis of the process of high-shear granulation was performed by Gantt et al.[12] The collision rate function was extracted from data gathered from several high-shear DEM simulations. The collision rate function extracted from the data was compared to the following existing kernels based on collision rate analysis: Equipartition of kinetic energy kernel (EKE), equipartition of translational momentum kernel (ETM), ortho-kinetic kernel (OK), peri-kinetic kernel (PK), and a size-independent kernel (SI). From analysis of extracted data, it was determined that the orthokinetic kernel best fit the simulation data for high-shear granulation. Therefore, the granule collision frequency caused by shear induced motion dominates over collisions due to random motion. The collision rate function used in this analysis is, therefore, defined by

$$C_{i,j} = \frac{1}{6} \Gamma (l_i + l_j)^3 \quad (8)$$

where Γ is the laminar shear rate and l_i is the diameter of particle i.

From results of the DEM simulations, an estimation for the coalescence efficiency, $\Psi_{i,j}$ can be made. During a simulation, the solid, liquid, and air volumes for both colliding particles are retained in a matrix A. Following each collision, criteria for Type I and Type II coalescence are calculated. A resulting vector b, stores a 1 for successful collisions, and 0 for unsuccessful collisions. Using the DEM data, a simple regression using the pseudo inverse of A can be used to map the collision information s_i, l_i, a_i, s_j, l_j, a_j, to a coalescence efficiency $\Psi_{i,j}$.

For clarity, solid, liquid, and air volumes are converted into more physically relevant terms: size $D = 2(3(s + l + a)/4\pi)^{1/3}$, pore saturation $S = (l/l + a)$ and porosity, $\varepsilon = (l + a/s + l + a)$. The equation for the linear regression is expressed as

$$\Psi_{i,j} = a_0 + a_1 D_{i,j} + a_2 S_{i,j} + a_3 \varepsilon_{i,j} \quad (9)$$

where $a_0 \cdots a_3$ are constants estimated from regression of simulation data $D_{i,j}$ is the mean size in meters of particles i and j. More complicated regressions, such as polynomial and hybrid regressions have been performed. For brevity, only the linear regressions are presented. A vector of coefficients $x = [a_0 \quad a_1 \quad \cdots \quad a_3]^T$ is solved using the pseudoinverse in the following manner

$$Ax = b$$

$$x = (A^T A)^{-1} A^T b \quad (10)$$

where A is an $N \times 4$ matrix of diameter, pore saturation, and porosity for N total collisions.

After combining Eqs. 8 and 9, the multiscale coalescence kernel used for this study is then

$$\beta_{i,j} = \zeta \frac{1}{6} \Gamma (l_i + l_j)^3 (a_0 + a_1 \bar{D}_{i,j} + a_2 \bar{S}_{i,j} + a_3 \bar{\varepsilon}_{i,j}) \quad (11)$$

where ζ is the fraction of collisions which have a ratio of the tangential to normal collision velocities which are greater than a critical number.

Adding dimensions to the problem increases the computational complexity required when solving the PBE. The following solution techniques have been used to solve PBEs:

- Analytical solutions to population balance equations are generally only available when the coalescence kernel is constant and therefore cannot be used for multidimensional cases.
- The method of moments typically results in a lower computational time. The method of moments also often involves the determination of fractional and negative moments depending on the kernel.[18] This requires the incorporation of extrapolation and interpolation techniques to solve the PBE.
- Sectional methods can be solved relatively quickly depending on the dimensionality of the problem. The algorithms required are complex, and resolution problems are typical. The sectional model can be significantly slowed when dealing with multidimensional modeling.[19] A sectional solution technique was applied for solving a multidimensional, volume-based PBE by Verkoeijen et al.[15] This approach was then adopted and modified to account for nonuniformally distributed liquid and air by Darelius et al.[20] This approach relies on an arithmetic

discretization of volume classes in the algorithm. An arithmetic distribution requires a large number of size classes to cover even a modest range of particle sizes. This results in a computationally demanding algorithm.

- Stochastic solution techniques require more computation time, but they allow for the accumulation of more data concerning collision history, internal structure, and inhomogeneity. Due to this, Monte-Carlo modeling is very well suited for discrete multidimensional modeling.[21] Stochastic techniques have been applied to derive a solution for multidimensional population balances by Wauters[16] and Goodson et al.[22]

Stochastic Solution Techniques

Typically Monte-Carlo (MC) modeling techniques can be subdivided into two categories: time driven and event driven. Event driven approaches select an appropriate event based on comparative probabilities. A time step is calculated for each event, based on the rates of the processes. Event driven MC, unlike time driven MC, does not require explicit time discretization. This makes the event driven algorithm preferential in many circumstances. Event driven MC can be further subdivided into two categories: *constant volume* and *constant number* approaches.

In constant volume MC, the total volume of the particles simulated is conserved. This means that number of particles is allowed increase due to breakage, or decrease due to coalescence. This method can lead to statistical inaccuracy when the number of particles is not sufficiently large enough to introduce a negligible error from the differentiation scheme.

The constant number MC developed by Smith and Matsoukas[23] alleviates the accuracy problems by maintaining the number of particles in the simulation constant, and the simulation volume is adjusted to account for changes due to breakage or coalescence. Due to the nature of the problem, particles can grow indefinitely. Similar solution methods are presented by Lee and Matsoukas,[24] Kostoglou and Konstandolopoulos[25] and Lin et al.[26] Constant volume MC would eventually not have enough particles to maintain accuracy. Furthermore, constant volume simulations where breakage events dominate can typically result in such a large number of particles that the simulation is slowed due to computational load.

Due to these advantages, constant number MC was applied to the stochastic modeling of the multidimensional population balance problem.

Constant Number Monte-Carlo Simulation

The development of the constant number MC algorithm is fully presented by Lin et al.[26] The algorithm used in this work is displayed in Algorithm 1.

This method is initialized by defining a distribution of solid s, liquid l, and air a, volumes for each particle in the array N. Only coalescence and consolidation will be taken into account, so the only discrete event will be coalescence. Particles are chosen at random from an array, and the probability of coalescence is determined.

A probability of coalescence $f_{i,j}$ is defined using the multidimensional coalescence kernel as

$$\Omega_{i,j} = \Omega_0 f_{i,j} = \zeta \frac{1}{6} \Gamma (l_i + l_j)^3 (a_0 + a_1 \bar{D}_{i,j} + a_2 \bar{S}_{i,j} + a_3^- \varepsilon_{i,j}) \tag{12}$$

or

$$f_{i,j} = (l_i + l_j)^3 (a_0 + a_1 \bar{D}_{i,j} + a_2 \bar{S}_{i,j} + a_3^- \varepsilon_{i,j}) \tag{13}$$

and

$$\Omega_0 = \zeta \frac{1}{6} \Gamma \tag{14}$$

where Ω_0 is the size independent portion of the multidimensional kernel.

The probability of coalescence $f_{i,j}$, will be a number between 0 and 1. If this number is larger than a random value uniformly distributed between 0 and 1, coalescence occurs. If not, two new random particles are selected and the process is repeated until a coalescence event occurs. It should be pointed out that while the probability of coalescence is variable, the fact that the value is constrained between 0 and 1 makes this MC approach more straightforward than when the coagulation frequency is an unconstrained function of the fractal dimension of the aggregate as found in 25.

When a coalescence event occurs, the volume of the new particle is simply defined as the sum of the constituent particle volumes; $s_1 + s_2 = s_3$, $l_1 + l_2 = l_3$, and $a_1 + a_2 = a_3$. This new particle replaces one of the constituent particles. The other constituent particle is replaced by a copy of a random particle from the array. Various authors have shown that when the array of particles is sufficiently large, the error introduced by the MC technique is negligible compared to simple analytical solutions.[23,24,26]

After a successful event is determined, the interevent time is calculated. This calculation considers an ensemble of particles which may undergo a number of differing events. The change in the number concentration due to an event, ΔC_k, is defined as

$$\Delta C_k = z_k \Delta t_k \sum_l R_l \tag{15}$$

where z_k is the change in the total amount of particles in event k, k is the total number of events, Δt is the change in time between events k and $k - 1$, and R is the rate of event l per unit time. In this example, the only discrete event is binary coalescence. Consequently, the change in the total number of particles z, is always -1. Smith and Matsoukas[23] define the total rate of coalescence of a system with a distribution of particles to be

$$\sum_l R_l = \frac{\Omega_0}{2} \int_0^\infty \int_0^\infty f_{i,j} c_i c_j d_i d_j = C_0 \frac{\langle f_{i,j} \rangle}{2\tau_c} \left(\frac{C}{C_0} \right)^2 \tag{16}$$

where τ_c is the characteristic coalescence time, defined as

$$\tau_c = \frac{1}{\Omega_0 C_0} \tag{17}$$

and $\langle f_{i,j} \rangle$ is the ensemble average kernel, which when discretized, is defined as

$$\langle f_{i,j} \rangle = \frac{2 \sum_{i=1}^{N} \sum_{j=i+1}^{N} f_{i,j}}{N(N-1)} \tag{18}$$

Again, note that $f_{i,j}$ will be a function of the particle sizes, pore saturations, and porosities determined following DEM analysis of the process. Combining Eqs. 15–18, Smith and Matsoukas[23] derived the final equation for the interevent time

$$\Delta t_k = \frac{2\tau_c}{\langle f_{i,j} \rangle} \frac{1}{N} \left(\frac{N}{N-1} \right)^k \tag{19}$$

For each simulation, given a known multidimensional kernel the process time can then be calculated.

Once the event time is calculated and the step is implemented, the change in air volume due to consolidation is updated. Consolidation has been modeled using a first-order rate equation for porosity reduction as described by Iveson et al.[27] as shown in Eq. 20

$$\frac{d\varepsilon}{dt} = -k(\varepsilon - \varepsilon_{min}) \tag{20}$$

where ε is the current porosity, k is a consolidation rate constant, and ε_{min} is the minimum porosity. Verkoeijen et al.[15] and Wauters[16] each derived a model for compaction behavior, based on the porosity definition in terms of solid, liquid, and air volumes. Given the relationship between porosity and air volume, Eq. 20 can be rewritten in terms of air loss assuming that solid and liquid volumes remain constant, and that only air escapes during the consolidation process. Rewriting the left-hand-side of Eq. 20 as a function of solid s, liquid l, and air a gives the following equation

$$\frac{d\varepsilon}{dt} = \frac{da}{dt} \frac{s}{(s+l+a)^2} \tag{21}$$

Combining Eq. 21 with the definition of porosity yields the following compaction rate equation as a function of s, l, and a

$$\frac{da}{dt} = -k \left(\frac{(l+a)(s+l+a)}{s} - \varepsilon_{min} \frac{(s+l+a)^2}{s} \right) \tag{22}$$

Since consolidation is a continuous process, this rate equation must be solved at each time step to determine the rate of air loss form each particle.

Algorithm Modifications

Accounting for induction

The process of consolidation slowly forces air out of the granule until a critical pore saturation is reached (assumed to be 0.85 for these simulations). Once this critical level is raised, any further consolidation slowly forces binder through pores to create a binder layer. Coalescence behavior is highly dependent on the formation of a binder layer. The period of inactivity leading to a binder layer formation is often called an induction period.[27,28] If the simulation is in an induction regime, there may not be any successful coalescence event among the possible collisions. This results in an infinite interevent time. In this case, the simulation will fail unless action is taken. While there may be no possible successful events at this point in time, consolidation will eventually result in the formation of a binder layer.

To alleviate this problem, an induction check step is added to the algorithm. Prior to the random selection of two particles for collision, the ensemble average kernel $\langle f_{i,j} \rangle$, is calculated. If there are no possible coalescence events at this time step, or the ensemble average is less than some tolerance δ, a *nonevent* event time is implemented. This event time Δt_{ind}, is equal to the previous successful time step. If no successful time steps have occurred $\Delta t_{ind} = 10^{-6}$ s. This allows consolidation and the time integration to occur as normal.

Rare-event simulation

The average probability of coalescence for high-shear granulation process described using parameters in Table 1 can be calculated from Eq. 13. This efficiency may vary somewhere between $f_{i,j} = 10^{-7}$, and $f_{i,j} = 10^{-8}$. Therefore, a successful collision occurs approximately once in every 10,000,000 to 100,000,000 collisions. This number is on the same order of magnitude as values proposed by Nilpawar et al.[29] for high-shear granulation. From an implementation point of view, it is highly computationally intensive and time consuming to require 10^7–10^8 random events per successful coalescence event. Straightforward simulations of this type may take days to run. This requires new implementation strategies to be considered. An analysis of rare-event stochastic processes is provided by Rubenstein.[30] To decrease the computation time, a minimum probability of coalescence was assumed to be: $f_{min} = 1 \times 10^{-8}$. The probability of coalescence is then normalized with respect to the minimum probability of coalescence $f_{new\ i,j} = f_{i,j}/f_{min}$. Therefore, the new probability is on the order 0.1. The size independent coalescence term is then redefined as

$$\Omega_0 = f_{min} \zeta \frac{1}{6} \Gamma \tag{23}$$

This allows the ensemble average probability of coalescence $\langle f_{i,j} \rangle$ to increase several orders of magnitude which speeds simulation time. This allows the time between events to be primarily dependent on the characteristic coalescence time $\tau_c = (1/f_{min}\zeta(1/6)\Gamma C_0)$. Implementation of this strategy speeds up the simulation to the order of seconds.

Case Study and Discussion

To test the applicability of this method for an experimental process, a simulation was performed to model high-shear granulation of lactose, starch, and hydroxy-propyl cellulose (HPC) with water as described by Sanders et al.[31] In this work, the powder and binder were mixed at 250 rpm and the granule-size

Table 1. DEM Simulation Conditions

Parameter	Value
Mean volume %, s, l, a	78, 16, 6
Solid density (lactose primarily), ρ_s	1000 [kg/m^3]
Liquid density (water), ρ_l	1000 [kg/m^3]
Liquid viscosity (water), μ_l	0.001 [kg/ms]
Number of particles, N_p	8000
Periodic boundary, ϕ	π/32 [rad]
Rotational speed of motor, ω	250 [rpm]

distribution was measured every 50 s by analysis of images taken inside the mixer. A DEM/coalescence model simulation was designed to match the experimental data provided in 31.

The initial granule-size distribution for the simulation was chosen to match the initial PSD found in 31. A 6% fraction of air was assumed to be present in the process initially. To maintain the same solid to liquid ratio, the new initial percentages are 78, 16, and 6 (% by volume) for solid, liquid, and air, respectively. As consolidation occurs, air will slowly escape.

The experimental data shows several interesting trends which should be taken into account when modeling the process. The first observation is that the particle-size distribution is narrowing with time. This is due to fact that the number of fines is decreasing with time and there are very few outlying large particles. Typically, processes which use low-viscosity binders, such as water are Type II coalescence dominated.[8] For a given set of parameters, Liu and Litster[8] observe that Type II coalescence is preferential towards larger particles. This creates a broadening of the PSD, which is not observed in this example. However, this observation is dependent on the operating conditions used for an experiment. A narrowing distribution is most often found in processes where Type I coalescence dominates. This is attributed to coalescence with viscous binders like oils. The goal is to find a set of operating conditions which describes this process.

One advantage of the DEM simulation technique is that parameters can be altered easily to determine what combination of parameters should produce the desired results. A process using water as a binder with a narrowing particle-size distribution was desired to replicate the given experimental data. Furthermore, the coefficient of restitution of the resulting collisions should be similar to findings by Mangwandi et al.[32] who measured the coefficient of restitution for wet granules, and reported values less than 0.2.

Several dimensionless groups used to define the coalescence criteria were used to fit MC simulated data to the experimental results. The dimensionless groups used were the ratio of the granule yield strength to the granule Young's modulus Y_d/E, and the ratio of the binder layer thickness to surface asperity thickness h_0/h_a. These groups are often not well defined and often vary several orders in magnitude in literature.[17]

Table 2. Simulations Chosen to Determine Which Simulation Parameters Most Closely Resemble Experimental Results

	Sim 1	Sim 2	Sim 3	Sim 4
Y_d/E^*	0.1	0.01	0.001	0.001
h_0/h_a	0.25	0.25	0.25	0.50
PSD result	widening	widening	widening	narrowing
mean e	0.99	0.48	0.19	0.19

Table 3. A List of Constants used in MC Simulation

Parameter	Value [unit]
Tangential collision efficiency factor, ζ	0.6 [-]
Shear rate, Γ	0.3 [s^{-1}]
Minimum coalescence probability, f_{min}	10^{-8} [-]
Coalescence constant, Ω_0	3.00e-10 [s^{-1}]
Minimum porosity, ε_{min}	0.29 [—]
Void fraction, ε_{void}	0.5 [—]
Compaction rate constant, k	0.0006 [s^{-1}]
Number of particles, N	10,000 [—]

To remain consistent with the experimental conditions used by Sanders et al.,[31] see Table 1 for a list of parameters for the simulations. Several simulations were then run with different sets of dimensionless parameters. This allowed for analysis of the resulting particle-size distribution, and to determine what sets of parameters produced realistic values for the coefficient of restitution. Simulation 4 produced a narrowing distribution with a mean coefficient of restitution of 0.19. This set of parameters was used to regress a coalescence kernel. See Table 2 for a summary of results.

Regression of DEM/Coalescence Model Data

To determine the coalescence efficiency for this set of parameters, a DEM/coalescence model simulation using the con-

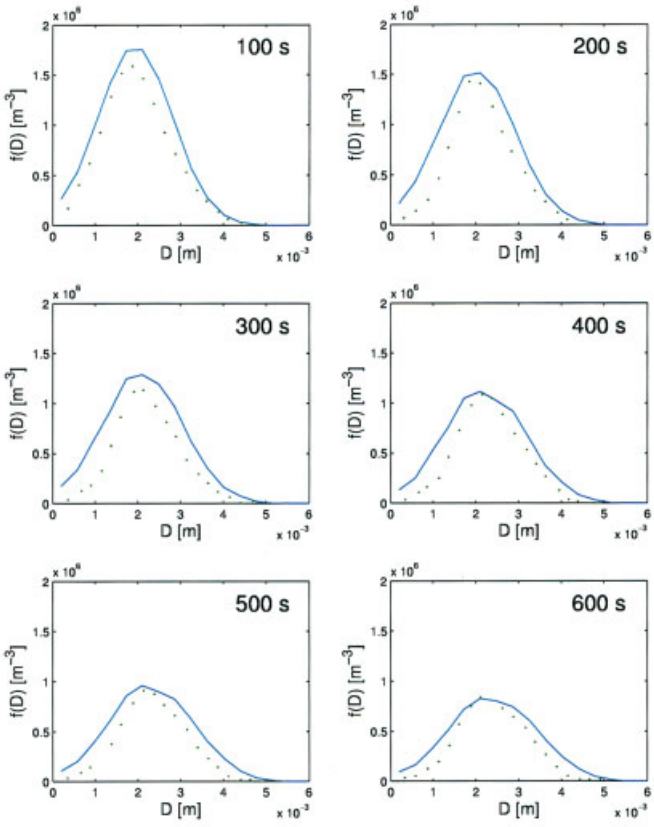

Figure 4. Experimental (●) and simulated (–) results found using the MC/DEM approach for a lactose/starch/HPC/water mixture.

[Color figure can be viewed in the online issue, which is available at www.interscience.wiley.com.]

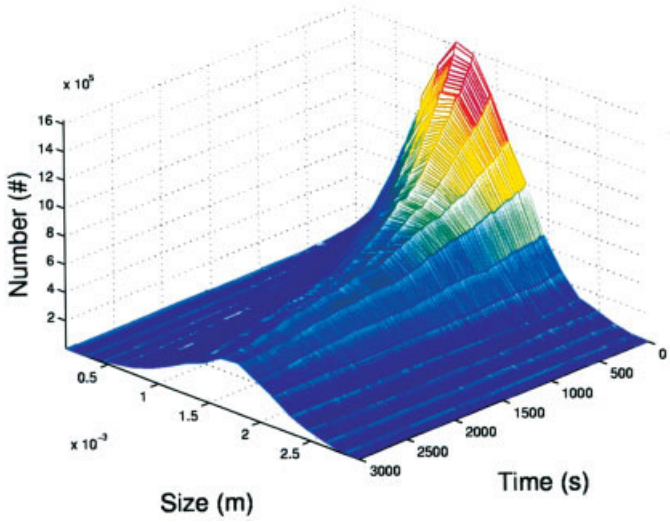

Figure 5. MC simulation results showing the evolution of the PSD after 3000 s.

[Color figure can be viewed in the online issue, which is available at www.interscience.wiley.com.]

ditions listed in Table 1 with $Y_d/E^* = 0.001$ and $h_0/h_a = 0.50$ was run. A regression was performed to determine coalescence efficiency dependence, based on internal coordinates for the two colliding particles. The kernel is then defined using Wauter's[16] definition of a multidimensional kernel

$$f_{i,j} = f_{min}(l_i + l_j)^3(-5.7 - 61.24\bar{D}_{i,j} + 6.15\bar{S}_{i,j} + 5.93\bar{\varepsilon}_{i,j}) \tag{24}$$

where f_{min} is the minimum coalescence efficiency defined earlier.

MC Simulation Results

Using the kernel found following a regression of DEM data, Monte-Carlo simulation was used in an attempt to replicate the high-shear experiment performed by Sanders et al.[31] The parameters used in the Monte-Carlo simulation are shown in Table 3. Sanders et al.[31] presents the number density $n(l)$, taken from experimentation. The number density was extracted from the MC simulation at each time-step by first determining the particle-size distribution at each step in the simulation from the known particle volumes. The number of particles at each size class N_c, and the total volume of particles V, are then used to determine the number density

$$f(D) = \frac{N_c}{V(1 + \varepsilon_{void})} \tag{25}$$

where ε_{void} is the void fraction of volume in the mixer.

To fit the results from the MC model to the experimental finding from Sanders et al.,[31] the tangential collision efficiency factor still must be estimated. This constant was created to account for the overestimated coalescence efficiency from the DEM/coalescence model. Therefore, this constant determines what fraction of particles actually coalesces and what fraction have a tangential velocity component which is too large for agglomeration. The constant which was found to best fit the experimental data is presented in Table 3.

The results for the Monte-Carlo simulation compared to the experimental data presented by Sanders et al.[31] are shown in Figure 4. The resulting particle-size distribution for the MC simulation is shown in Figure 5. The MC simulation corresponds well with the experimental data. The simulation presented here did not experience induction. This shows that there was sufficient binder present to form a binder layer. In fact, these results show that the process was primarily in a rapid-growth regime. Since the kernel shows that coalescence probability is inversely proportional to particle size, there is a final narrowing distribution which the simulation approaches. Sim-

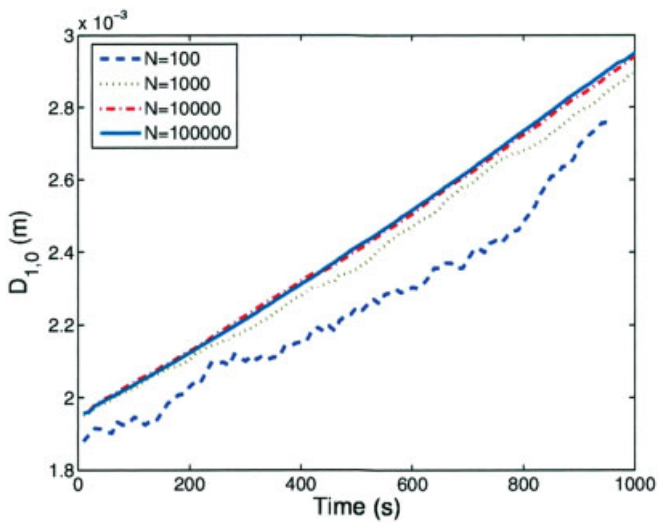

Figure 6. Sensitivity analysis for the MC simulation to determine how the number of particles in the simulation affects agglomeration.

[Color figure can be viewed in the online issue, which is available at www.interscience.wiley.com.]

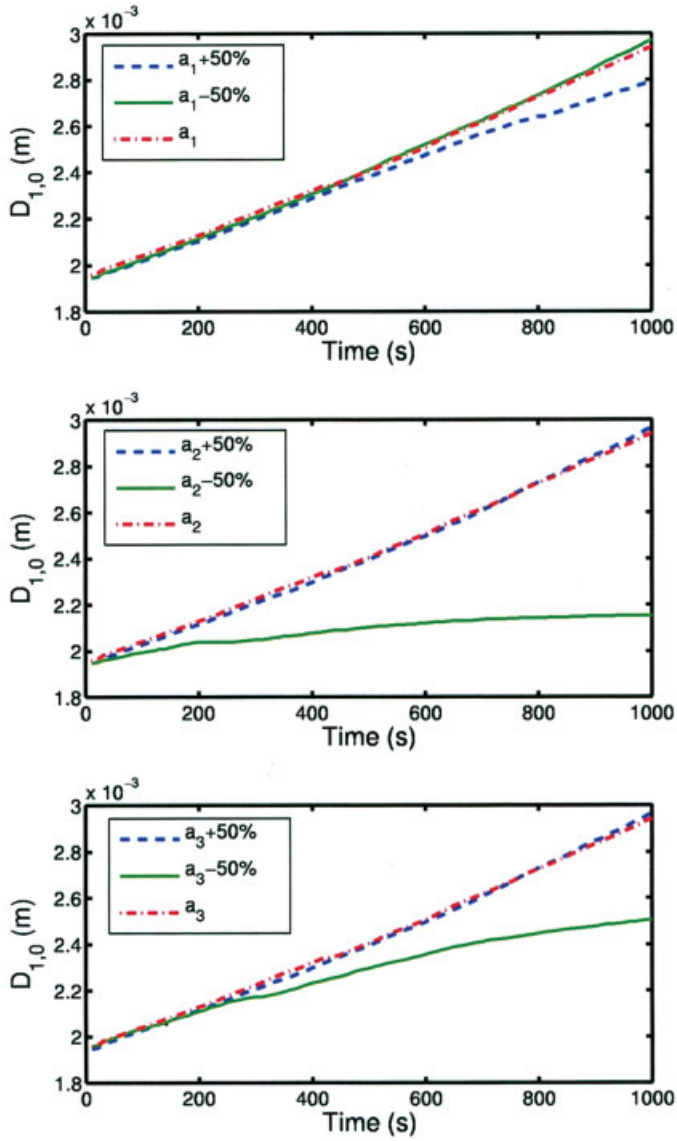

Figure 7. Parametric analysis of the MC algorithm analyzing changes in the particle size term a_1, the pore saturation term a_2, and the porosity term a_3.

[Color figure can be viewed in the online issue, which is available at www.interscience.wiley.com.]

ilar observations have been illustrated by Adetayo et al.[33] when performing Stokes regime analysis. The analysis explains that rapid growth occurs in the "*non-inertial*" regime where $St \ll St^*$ until particles reach a critical size where the "*coating*" regime begins and the PSD remains constant.

While the PSD in Figure 5 appears continuous, it should be pointed out that it is not indeed smooth. In fact, it is noisy due to the stochastic nature of the simulation, but due to the average length of the time steps taken (~0.04 s) the distribution appears to be smooth.

Sensitivity analysis

A sensitivity analysis was also performed with respect to the total number of particles in the simulation to determine how the number of particles affect the extent of agglomeration. For a simulation with 10,000 particles the mean particle size $D_{1,0} = 2.404$ mm, the number concentration, $C = 4.884 \times 10^6$ m^{-3}, and the standard deviation of the array of particles $St_{dev} = 0.991$ mm. These values were then extracted for simulations of 100, 1,000, and 100,000 particles. From the results of the sensitivity analysis it is clear that a simulation with 10,000 particles is accurate to within a one percent error of a simulation with 100,000 particles for each of the parameters selected. Only the simulation with 100 particles produced results with errors greater than three percent. Furthermore, as the number of particles decreases, the stochastic nature of the simulation becomes more evident. Figure 6 shows the evolution of the mean particle size for each of the simulations.

Parametric analysis

To conclude this work a parametric analysis was performed to demonstrate the utility of this simulation technique. Each

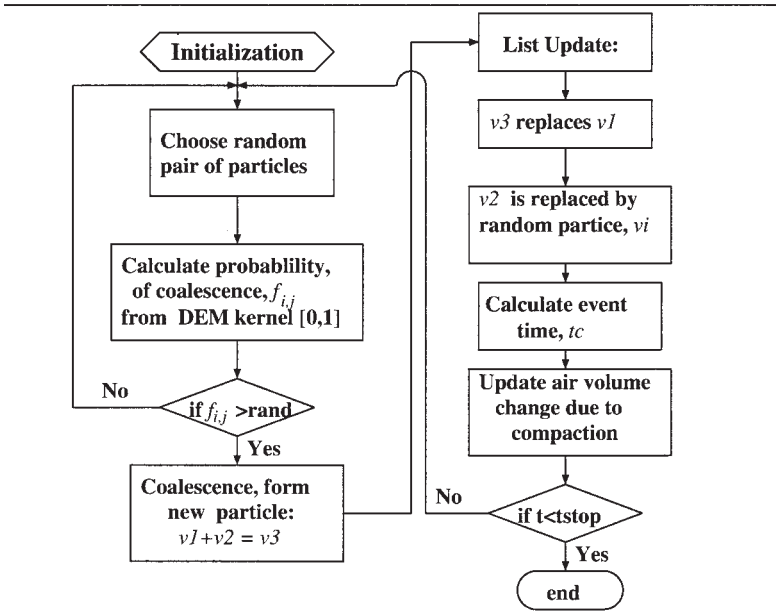

Algorithm 1. Constant number Monte-Carlo algorithm used for solving multidimensional PBE problem.

individual case study will result in a different set of regressed coefficients for the coalescence efficiency depending on wet granule parameters, such as Young's modulus, granule yield strength, and binder viscosity. A change in any of these parameters will result in a different evolution of the particle-size distribution. In this work, parametric analysis was performed where the parameters a_1, pertaining to particle size a_2, pertaining to pore saturation, and a_3, pertaining to porosity are increased and decreased by 50% from their nominal value, which in this case is taken from the case study in Eq. 24. Figure 7 shows this how changes in each of these parameters affect the evolution of the mean-particle size. Increasing the particle size term, a_1, makes the term more negative, therefore decreasing the probability of coalescence for large particles. Decreasing both a_2 and a_3 have similar effects as they drastically decrease the rate of coalescence. It should be pointed out that this effect is not symmetric. Increasing a_2 and a_3 have little effect on particle growth. Therefore, the case study presented a simulation where the rate of agglomeration was almost a maximum.

Conclusions

In this work, a multidimensional population balance was solved using a constant number Monte-Carlo simulation approach. The kernel used was unique because it was based on multiscale analysis of data extracted from a discrete element simulation of a high-shear granulation process. The coalescence model used accounted for a viscous binder layer and deformation caused by collisions, making it one of the most physically relevant simulations available in literature. The Monte-Carlo simulation was found to be good agreement with experimental results.

Despite this success, the coupling of the DEM simulation and the MC simulation is not trivial. There are still many parameters which are unknown. Therefore, additional information must be determined for wet granule yield strength, Young's modulus, and asperity height for this method to be even more effective.

It is now well understood that modeling of particulate processes require more than just a simple size-dependent model to capture dynamic affects of pore saturation, moisture content and porosity due to the consolidation process. This model creates a bridge between the microscale modeling of particulate interactions using DEM and coalescence modeling to the mesoscale population balance models. This article shows that Monte-Carlo algorithms prove to be effective tools in solving multidimensional PBEs. When linking this with knowledge of particle interactions provided by DEM simulations, this method can prove to be a realistic means of modeling the complex dynamic mechanisms observed in granulation processes.

Table 4. Sensitivity Analysis for the MC Algorithm

	$N \times 10^{-2}$	$N \times 10^{-1}$	$N \times 10^{1}$
$D_{1,0}$ (mm)	−8.50%	−2.12%	+0.42%
C (m^{-3})	+20.56%	+1.53%	−0.08%
St_{dev}	+13.27%	−1.22%	−0.92%

Notation

a = air particle volume, m^3
C_k = number concentration of granules at event k, m^{-3}
D = particle diameter, m
e = coefficient of restitution
E = particle Young's modulus, N/m^2
$f_{A,B}$ = probability of coalescence
k = rate of compaction, s^{-1}
l = liquid particle volume, m^3
m = particle mass, kg
n = number density function, m^{-9}

R_l = rate of event l, s^{-1}
s = solid particle volume, m^3
S = particle pore saturation
St_v = viscous Stokes' number
St_{def} = Stokes' deformation number
Δt = time step, s
z_k = change in the number of particle at event k

Greek letters

β = 1-D coalescence kernel
ζ = tangential collision rejection factor
ε = particle porosity
ε_{void} = void fraction
Γ = laminar shear rate, s^{-1}
μ = binder viscosity, kg/m/s
τ_c = characteristic coalescence time
Ω = multidimensional coalescence kernel

Literature Cited

1. Iveson, SM. Limitations of one-dimensional population balance models of wet granulation processes. *Powder Technol.* 2002;124:219–229.
2. Kapur PC, Fuerstenau DW. Coalescence model for granulation. *Ind and Eng Chem Proc Design Devices.* 1969;8:56–62.
3. Sastry KVS. Similarity size distribution of agglomerates during their growth by coalescence in granulation or green pelletization. *Intl J of Mineral Processing.* 1975;2:187–203.
4. Adetayo AA, Ennis BJ. A unifying approach to modeling coalescence mechanisms. *AIChE.* 1997;43(1):927–934.
5. Iveson SM, Beathe JA, Page NW. The dynamic strength of partially saturated powder compacts: the effect of liquid properties. *Powder Technol.* 2002;127:149–161.
6. Liu LX, Litster JD. Coalescence of deformable granules in wet granulation processes. *AIChE J.* 2000;46(3):529–539.
7. Liu LX, Litster JD, Iveson SM, Ennis BJ. Coalescence of deformable granules in wet granulation processes. *AIChE J.* 2000;46(3):529–539.
8. Liu LX, Litster JD. Population balance modeling of granulation with a physically based coalescence kernel. *Chem Eng Sci.* 2002;57:2183–2191.
9. Tsuji T, Kawaguchi T, Tanaka T. Discrete particle simulation of two-dimensional fluidized bed. *Powder Technol.* 1993;77:79–87.
10. Muguruma Y, Tanaka T, Tsuji Y. Numerical simulation of particulate flow with liquid bridge between particles (simulation of centrifugal tumbling granulator). *Powder Technol.* 2000;109:49–57.
11. Cundall PA, Strack ODL. A discrete numerical model for granular assemblies. *Geotechnique.* 1979;29:47–65.
12. Gantt JA, Cameron IT, Litster JD, Gatzke EP. Determination of coalescence kernels for high shear granulation using dem simulations; 2005.
13. Goldshmidt M. *Hydrodynamic Modelling of Fluidized Bed Granulation.* Twente University, 2001. PhD thesis.
14. Tan H, Goldschmidt M, Boerefijn R, Hounslow M, Salman A, Kuipers J. Building population balances for fluidized bed granulation: lessons from kinetic theory of granular flow. *Powder Technol.* 2004;142(30):103–109.
15. Verkoeijen D, Pouw GA, Meesters GMH, Scarlett B. Population balances for particulate processes—a volume approach. *Chem Eng Sci.* 2002;57:2287–2303.
16. Wauters P. *Modeling and mechanisms of granulation.* Delft University of Technology, Delft, The Netherlands; 2001. PhD thesis.
17. Ingram GD. *Multiscale Modeling and Analysis of Process Systems.* University of Queensland, St. Lucia, Queensland, AU; 2006. PhD thesis.
18. Diemer R, Olson J. A moment methodology for coagulation and breakage problems: Part 1—analytical solution of the steady state population balance. *Chem Eng Sci.* 2002;57:1735–1742.
19. Hounslow MJ, Ryall RL, Marshall VR. A discretized population balance for nucleation, growth and aggregation. *AIChE J.* 1988;34(11):1821–1832.
20. Daralius A, Brage H, Rasmusson A, Bjorn I, Folestad S. A volume-based multidimensional population balance approach for modelling high shear granulation. *Chem Eng Sci.* 2006;61:2482–2493.
21. Das P. Monte carlo simulation of drop breakage on the basis of drop volume. *Comp and Chem Eng.* 1995;20(3):307–313.
22. Goodson M, Kraft M, Forrest S, Bridgewater J. A multi-dimensional population balance model for agglomeration. In *PARTEC;* 2004.
23. Smith M, Matsoukas T. Constant-number monte carlo simulation population balances. *Chem Eng Sci.* 1998;53(9):1777–1786.
24. Lee K, Matsoukas T. Simultaneous coagulation and break-up using constant-n monte carlo. *Powder Technol.* 2000;110:82–89.
25. Kostoglou M, Konstandolopoulos A. Evolution of aggregate size and fractal dimension during brownian coagulation. *J of Aerosol Sci.* 2001;32:1399–1420.
26. Lin Y, Lee K, Matsoukas T. Solution of the population balance equation using constant-number monte carlo. *Chem Eng Sci.* 2002;57:2241–2252.
27. Iveson S, Litster J, Ennis B. Fundamental studies of granule consolidation. part 1: effects of binder content and binder viscosity. *Powder Technol.* 1996;88:15–20.
28. Iveson SM, Litster JD, Hapgood K, Ennis BJ. Nucleation, growth and breakage phenomena in agitated wet granulation process: a review. *Powder Technol.* 2001;117:3–39.
29. Nilpawar A, Reynolds G, Salman A, Hounslow M. Kinematics in high shear granulation. In *Proceedings: The 8th International Symposium on Agglomeration,* 447 Sri Ayudhaya rd. Bangkok, Thailand, 2005. The Industrial Pharmacists Group.
30. Rubinstein RY. Optimization of computer simulation models with rare events. *Euro J of Operational Res.* 1997;99:89–112.
31. Sanders C, Willemse A, Salman A, Hounslow M. Development of a predictive high shear granulation model. *Powder Technol.* 2003;138:18–24.
32. Mangwandi C, Fu J, Reynolds G, Adams M, Hounslow M, Salman A. Impact behavior of different types of granules. In *8th International Symposium on Agglomeration,* Sri Ayudhaya rd, Bangkok, Thailand, The Industrial Pharmacists Group. 2005; p 11–21: 447.
33. Adetayo AA, Ennis BJ. A new approach to modeling granulation processes for simulation and control purposes. *Powder Technol.* 2000;108:202–209.

Manuscript received Oct. 16, 2005, and revision received May 3, 2006.